

# Nanostructuring of TiNi Alloy by SPD Processing for Advanced Properties

Ruslan Valiev<sup>1,\*</sup>, Dmitry Gunderov<sup>1</sup>, Egor Prokofiev<sup>1</sup>, Vladimir Pushin<sup>2</sup> and Yuntian Zhu<sup>3</sup>

<sup>1</sup>Institute of Physics of Advanced Materials, Ufa State Aviation Technical University, 12 K. Marx str., Ufa 450000 Russia

<sup>2</sup>Institute of Metal Physics, Ural Division of Russian Academy of Sciences, 18 S. Kovalevskaya str., Ekaterinburg 620219 Russia

<sup>3</sup>Department of Materials Science and Engineering, North Carolina State University, Raleigh, NC 27695-7919 USA

Ultrafine-grained (UFG) alloy Ti<sub>49.4</sub>Ni<sub>50.6</sub> possessing both nano- as well as submicrocrystalline structure has been successfully produced using two techniques of severe plastic deformation (SPD) processing: high pressure torsion and equal channel angular pressing. The features of microstructure, martensitic transformation and deformation behavior of the UFG alloy have been studied in details. The effects of grain size on the mechanical and functional properties of the alloy are discussed. [doi:10.2320/matertrans.ME200722]

(Received August 10, 2007; Accepted October 23, 2007; Published December 12, 2007)

**Keywords:** severe plastic deformation, ultrafine grains, mechanical properties, shape memory titanium nickel alloy

## 1. Introduction

TiNi alloys are well-known thanks to their remarkable properties—enhanced strength, corrosion resistance, and especially superelasticity and shape-memory effect. Due to this, they are very promising for many structural and functional applications in engineering and medicine.<sup>1–3)</sup> Superelasticity and shape-memory effect of TiNi alloys are associated with martensitic transformations (MT) of the austenite phase B2 into the martensite phase B19'. These two extraordinary properties have been the object of numerous fundamental investigations. At the same time, for various advanced applications superior properties of TiNi would be very desirable, since they are required for miniaturization of articles and enhancement of their functional characteristics. Recent investigations testify that an effective way to enhance the properties of various metals and alloys is their nanostructuring using severe plastic deformation (SPD) processing.<sup>4–6)</sup>

During last years in our laboratories a number of investigations have been performed, dealing with nanostructuring of TiNi alloys,<sup>7–11)</sup> using two most popular SPD techniques—high-pressure torsion (HPT) and equal-channel angular pressing (ECAP), and with the effect of the formed nanostructure on the deformation behaviour of alloys and martensitic transformations. This paper reports the results of the investigations of mechanical and functional properties of the Ti<sub>49.4</sub>Ni<sub>50.6</sub> alloy that has an ultrafine-grained structure in the nano- and submicrocrystalline ranges.

## 2. Experimental Procedure

The Ti<sub>49.4</sub>Ni<sub>50.6</sub> alloy supplied by Intrinsic Devices Inc. (USA) was used as an initial material for investigations. The temperature Ms of martensitic transformation B2 (austenite) → B19' (martensite) of the Ti<sub>49.4</sub>Ni<sub>50.6</sub> alloy quenched from 800°C is about 15°C. The alloy has the austenite structure at room temperature. The alloy with submicrocrystalline structure was produced by ECAP at  $T = 450^\circ\text{C}$ , intersection angle  $\Phi = 110^\circ$ , the number of

passes  $n = 8$ .<sup>7)</sup> The nanocrystalline alloy was processed by HPT with consequent annealings at various regimes (see below). Straining and annealing were conducted in the open air. Microstructure of the samples after processing was studied by TEM and X-ray.

The tensile tests at room temperature were carried out on flat small samples with a gage of  $1 \times 0, 25 \times 3$  mm and a rate of extension  $3 \cdot 10^{-4} \text{ s}^{-1}$  using a specially designed tensile machine<sup>12)</sup> and dynamometer “Instron” on standard cylindrical samples with a gage 3 mm in diameter and 15 mm in length. The dimensions of these samples enabled to cut the thin foils both in cross and longitudinal sections meant for TEM investigations of the material after tensile testing.

## 3. Results

The microstructural features and properties of the alloy with a nano- and submicrocrystalline structure will be considered separately below.

### 3.1 Nanocrystalline TiNi (nc-alloy)

As was noted above, the nc-alloy was produced using HPT. The processing was carried out with an original HPT unit that enables processing of samples with larger dimensions, in the form of disks Ø20 mm and with thickness 0.8 mm.<sup>11)</sup> The applied pressure was 6 GPa, and the number of revolutions totaled 5. After this processing, as we observed earlier,<sup>8,13)</sup> almost complete amorphization occurs in the alloy.

Investigations showed that ultimate tensile strength (UTS) of the samples immediately after HPT exceeded 2000 MPa, while their ductility made approximately 7% (Fig. 1). At that the flow curve did not show the area of phase pseudo-yield, which results from the absence of stress-induced martensitic transformation in the amorphized TiNi.

According to TEM analysis, the samples subjected to HPT acquire uniform NC structure with an average size of grains of about 20 nm when annealed at 400°C for 20 min or 1 hour (Fig. 2).

It is interesting to note, that after annealing at the temperature 400°C and higher irrespective of the specified hold time the stress-strain curves indicate the appearance of

\*Corresponding author, E-mail: RZValiev@mail.rb.ru.

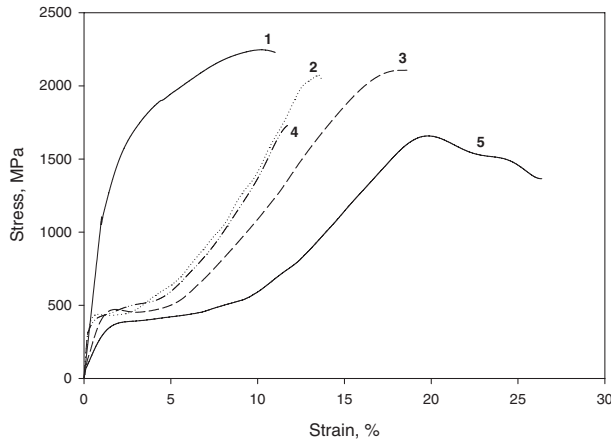


Fig. 1 Engineering stress-strain curves for TiNi samples subjected to HPT and subsequent annealing: *curve 1*—not annealed, *curve 2*—annealed at 400°C (5 min), *curve 3*—annealed at 400°C (20 min), *curve 4*—annealed at 400°C (1 h), *curve 5*—annealed at 450°C (20 min).

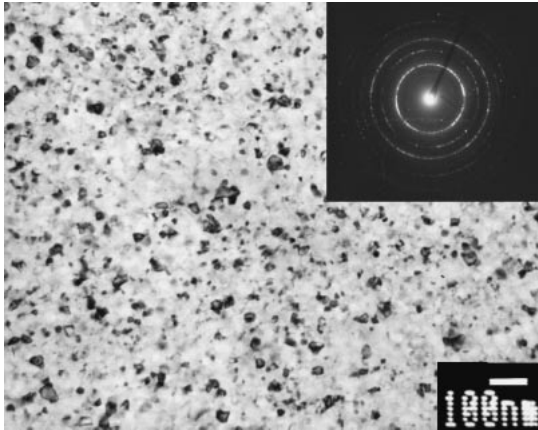


Fig. 2 TEM image of the TiNi alloy processed by HPT ( $n = 5$ ) and annealed at 400°C (1 h).

the area of phase pseudo-yield (Fig. 1), which is connected with the formation of nanocrystalline B2 phase structure, capable of stress-induced martensitic transformation (MT). The extension of the stress-strain curve area, preceding the linear stage of strain hardening of true martensite and on which the martensitic transformation in the sample is fully completed, varies constituting 5% and more (curves 2–5) depending on the annealing regime.

The samples processed by HPT and annealed at the temperature of 400°C (1 h) did not reach UTS and dislocation yield and showed brittle fracturing under stress of 1750 MPa. By cutting the time of annealing during the formation of NC structure, it became possible to increase the ductility of the samples subjected to HPT processing. In particular, the samples annealed at 400°C for 5 minutes and 20 minutes demonstrated ductility amounting to 12 and 16% and strength over 2000 MPa (see Fig. 1). Thus, the 1-hour annealing of the HPT-processed samples at the temperature of 400°C introduces brittle behavior in the alloy. Meanwhile shorter-time annealing (20 min. and 5 min.) at the same temperature

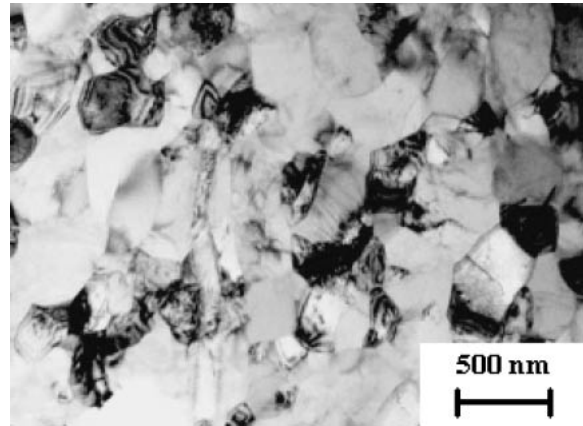


Fig. 3 Microstructure of smc  $Ti_{49.4}Ni_{50.6}$  processed by ECAP (cross section).

increases the ductility of NC TiNi while retaining high level of its strength characteristics. We believe that there might be possibly a connection of brittle fracturing with aging processes (heterogeneous precipitation of phases enriched with nickel- $Ti_3Ni_4$  и  $Ti_2Ni_3$ <sup>14</sup>) taking place along the boundaries of nanograins with increase of time of annealing up to one hour and more but not yet marked at shorter annealings. Presently we study this phenomenon in details.

### 3.2 Submicrocrystalline TiNi (smc-alloy)

The smc-alloy was produced using ECAP. ECAP processing of TiNi alloys cannot be carried out at room temperature due to their low deformability, therefore their processing was performed at 450°C.<sup>7,10</sup>

The quenched  $Ti_{49.4}Ni_{50.6}$  alloy at room temperature had an austenite structure with a grain size of about 50  $\mu m$ —coarse-grained (CG) state. After ECAP the alloy also had an austenite structure with both equiaxed grains/subgrains (Fig. 3). Most grains are free from dislocations or their density is rather small. The average size of grains/subgrains in the cross section equals to about 300 nm. Grains in the longitudinal section are somewhat elongated.

Figure 4 shows engineering stress-strain curves of CG and smc  $Ti_{49.4}Ni_{50.6}$  alloy measured at different testing temperatures. The main feature of the stress-strain curves for room temperature of CG and smc TiNi is the presence of an extended region of uniform deformation up to 70–80%. However their value of yield stress considerably varies. Moreover, in both alloys there observed a “plateau” attributed to the stress-induced martensitic transformation but the magnitude of stress ( $\sigma_m$ ) of pseudo-yield for the smc alloy is considerably higher than that for the CG alloy. At 200°C the yield stress of smc alloy is also by almost two times higher than of CG alloy. At 400°C the strength of both CG and smc alloy is considerably decreased. It appears that tension of the alloy at the temperatures above 200°C could not induce martensitic transformation because the curves  $\sigma(\epsilon)$  of both CG and smc alloys do not have the stage of phase pseudo-yield. At 200 and 400°C the strengthening stage of both states is quickly replaced by a softening stage and a stage of neck formation. As a result, the total strain to failure of both CG and smc alloys considerably decreases.

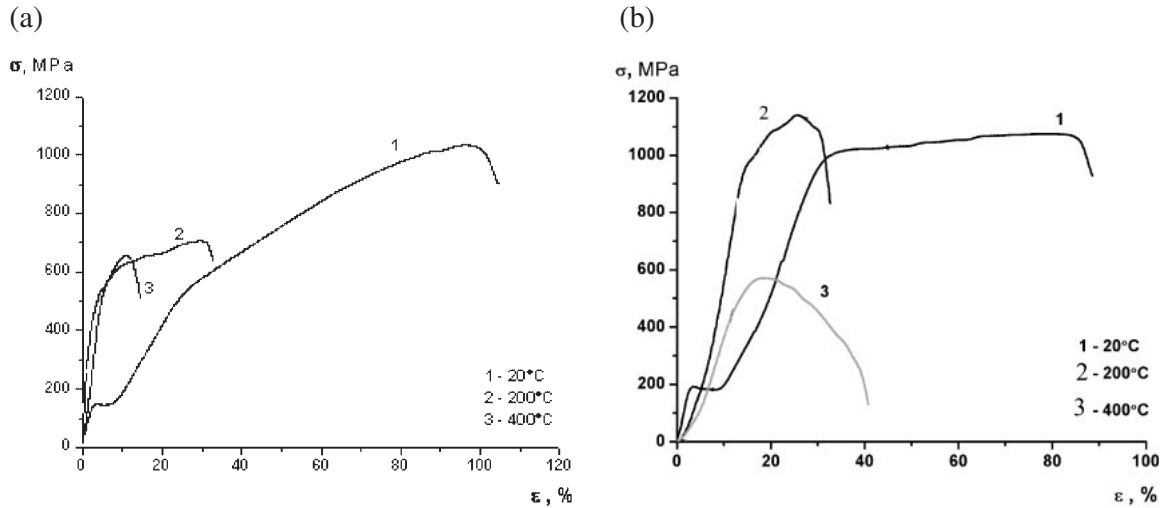


Fig. 4 Engineering stress-strain curves for  $\text{Ti}_{49.4}\text{Ni}_{50.6}$  at different temperatures: (a) CG state; (b) smc state.

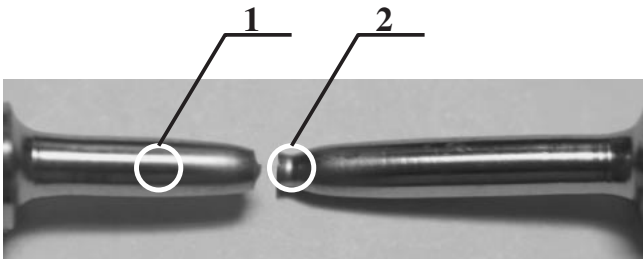


Fig. 5 General view of gauge section of a  $\text{Ti}_{49.4}\text{Ni}_{50.6}$  sample with a base of  $\text{Ø}3 \times 15$  mm after mechanical testing: (1) region of uniform deformation; (2) neck region.

Thus, both CG and smc alloys demonstrate very high ductility with elongation to failure constituting more than 70% (Fig. 5) during tension at room temperature. As it is known, in CG alloys this ductility is attributed to the considerable strain hardening right after the “plateau” stage. At the same time high ductility in smc alloys is accompanied by high strength–dislocation yield stress of the smc TiNi equals to  $YS = 990$  MPa, which is almost two times higher than the same value of the CG alloy. This is a rather unusual result as the ductility of ultrafine-grained metals is commonly not very high and does not exceed 10%.<sup>15,16</sup> Alongside with that, the ductility suddenly and considerably decreases in the smc alloy with the increase of test temperature, when the “plateau” disappears, which testifies to the fact that high ductility of the alloy is obviously in close connection with stress-induced martensitic transformation. The suppression of this transformation at higher temperatures leads to the considerable change in deformation behaviour of the alloy.

The microstructure of CG samples after tension in the region of uniform deformation ( $\epsilon \approx 40\%$ ) is shown in Fig. 6(a) (area shown in Fig. 5, “1”). A band substructure is observed both in longitudinal and cross sections of tensile samples and this substructure is oriented in different grains along one or several slip systems. The density of dislocations homogeneously distributed in the bands is so high that individual dislocations are not visible practically. The SAED

patterns exhibit spots of both B2-austenite and B19'-martensite. It appears that fully martensitic state was formed in the process of the tension of the alloy. However, after unloading of the tensile sample a reverse martensitic transformation  $\text{B19}' \rightarrow \text{B2}$  took place in the alloy in accordance with its critical temperatures, but obviously only partially because the transformation can be suppressed by the increased defect density and residual internal stresses.<sup>14,17</sup>

The smc alloy after tension in the uniform gage region has almost one B2-phase (Fig. 6(b)). Insignificant amount of the martensite could be only revealed in this region after tension. This observation indicates that practically the complete reverse martensitic transformation takes place after unloading and therefore superelasticity of this alloy should be essentially higher. This assumption is in good agreement with the recent direct measurements of functional properties—recoverable strain and reactive stress in TiNi alloys after various treatments<sup>7,10</sup> which demonstrated that these values are considerably higher in the smc state than in CG alloy.

However, the microstructure in the necking area (Fig. 7) has changed considerably. The microstructure is strongly refined and is mainly of the martensite type. Microstructure has nanotwin packets and bands of 20–40 nm thick. Dislocation density is very high. It appears that the stress-induced martensite did not transform back into austenite after unloading here. Thus, such microstructure results from martensitic transformation and apparently has a direct influence on deformation behavior of the smc alloy.

#### 4. Discussion

The conducted experiments demonstrate that SPD processing enables to achieve successfully the ultrafine-grained (UFG) structure within the nano- and submicrocrystalline ranges in TiNi alloys. The formation of UFG structure produces a considerable effect on deformation behavior and properties of the alloys.

The NC  $\text{Ti}_{49.4}\text{Ni}_{50.6}$  alloy with the grain size of 20–30 nm exhibits very high strength, exceeding 2000 MPa, but has low ductility, which apparently attributes to the effects of ageing



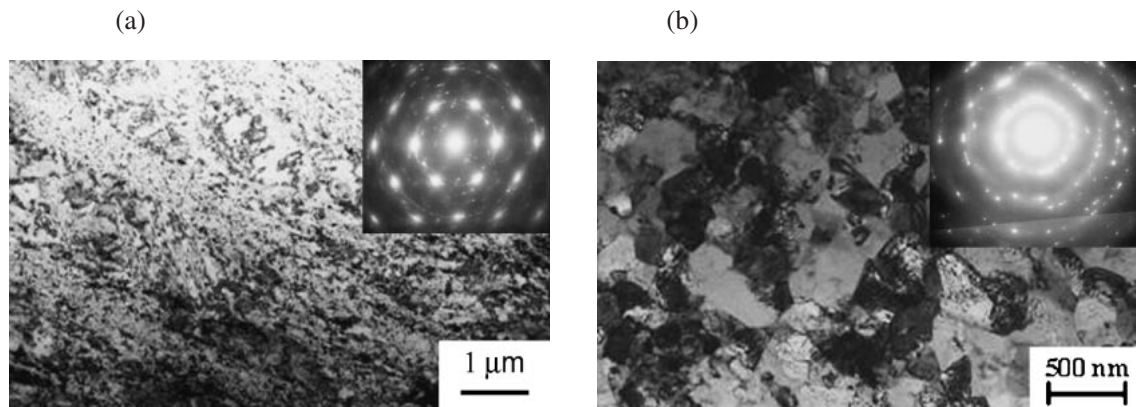


Fig. 6 TEM image of the CG  $\text{Ti}_{49.4}\text{Ni}_{50.6}$  alloy after tension (40%): CG (a) and smc (b) states (cross section).

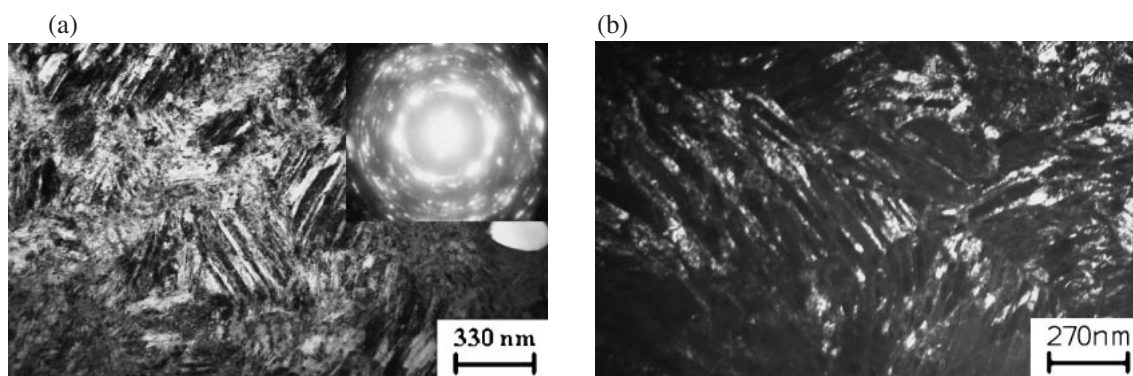


Fig. 7 Microstructure of the smc  $\text{Ti}_{49.4}\text{Ni}_{50.6}$  after tension in the necking area, bright (a) and dark-field (b) (cross section).

at grain boundaries. As it is known<sup>18)</sup> the martensitic transformation is suppressed in NC TiNi alloys at cooling. However, in the present work the stress-induced martensitic transformation takes place in this alloy indicating that NC alloy may combine high-strength state and good functional properties.

Submicrocrystalline alloy demonstrates rather unusual combination of high strength with  $\text{UTS} \geq 1200 \text{ MPa}$  and high ductility at room temperature. The obtained results show that such ductility of the alloy is in close connection with the stress-induced martensitic transformation as the increase of strain temperature, suppressing the martensitic transformation, leads to a considerable decrease of ductility.

In recent years the unusual combination of very high strength and ductility revealed in several UFG metals and alloys has become the subject of intensive research in a whole number of works.<sup>15,19–21)</sup> It was demonstrated that the formation of second phases, creation of bimodal structure or formation of special grain boundaries<sup>5)</sup> contribute to the enhancement of ductility of UFG materials while keeping the high strength. In particular, the introduction of twinings into UFG copper by means of rapid cooling<sup>20)</sup> or rolling at very low temperature<sup>21)</sup> enables to achieve its record high strength and ductility. The nature of this effect is connected with the influence of twinings on the strain hardening, which contributes to the delay of strain localization and enhancement of flow stability. Apparently, similar nature refers to the origin of high ductility in the smc TiNi alloy. As it was

demonstrated above, during tension of the alloy at room temperature the stress-induced martensitic transformation leads to the appearance of twins and martensitic plates inside the fine grains of high density, which then contributes to the accumulation of dislocation density during straining and provides the enhancement of strain hardening.

Thus, the nanostructuring of the TiNi alloy by means of SPD processing enables to considerably influence its properties. The reduction of grain size up to nanometer range and control of the development of martensitic transformation provide the opportunity to considerably enhance both mechanical as well as functional properties of TiNi alloys, which is very promising for application of these alloys in medicine and engineering.

### Acknowledgements

The present work was partly supported by the ISTC #3208 project through the IPP-DOE program and grants of the Russian Ministry of Education and Science.

### REFERENCES

- 1) K. Otsuka and C. M. Wayman (eds.): *Shape Memory Materials*, (Cambridge: Cambridge University Press, 1999) p. 284.
- 2) V. Brailovski, S. Prokoshkin, P. Terriault and F. Trochu (eds.): *Shape Memory Alloys: Fundamentals, Modeling and Applications*, (Montreal: ETS Publ., 2003) p. 851.
- 3) D. M. Brunette, P. Tengvall, M. Textor and P. Thomsen: *Titanium in*

- Medicine*, (Springer-Verlag Berlin Heidelberg, 2001) p. 1019.
- 4) R. Z. Valiev, R. K. Islamgaliev and I. V. Alexandrov: *Prog. Mater. Sci.* **45** (2000) 103–189.
  - 5) R. Z. Valiev: *Nature Mater.* **3** (2004) 511–516.
  - 6) Z. Horita (ed.): *Proc. 3rd Int. Conf. on Nanomaterials by Severe Plastic Deformation*, (Trans Tech Publications LTD, Switzerland, 2006).
  - 7) V. V. Stolyarov, E. A. Prokofyev, S. D. Prokoshkin, S. V. Dobatkin, I. B. Trubizina, I. Y. Khmelevskaya, V. G. Pushin and R. Z. Valiev: *Phys. Met. Metallogr.* **100** (2005) 608–618.
  - 8) V. G. Pushin, D. V. Gunderov, N. I. Kourov, L. I. Yurchenko, E. A. Prokofiev, V. V. Stolyarov, Y. T. Zhu and R. Z. Valiev: *Ultrafine grained materials III*, (TMS, Charlotte: NC, USA, 2004) pp. 481–486.
  - 9) J. Y. Huang, Y. T. Zhu, X. Z. Liao and R. Z. Valiev: *Phil. Mag. Letters.* **84** (2004) 183–190.
  - 10) V. G. Pushin, R. Z. Valiev, Y. T. Zhu, S. D. Prokoshkin, D. V. Gunderov and L. I. Yurchenko: *Proc. 3rd Int. Conf. on Nanomaterials by Severe Plastic Deformation*, ed. by Z. Horita, (Trans Tech Publications LTD, Switzerland, 2006) pp. 539–544.
  - 11) D. V. Gunderov: *Phys. Met. Metallogr.*, to be published.
  - 12) O. B. Kulyasova, R. K. Islamgaliev and R. Z. Valiev: *Phys. Met. Metallogr.* **100** (2005) 277–283.
  - 13) R. Z. Valiev, A. V. Sergueeva and A. K. Mukherjee: *Scripta Mater.* **49** (2003) 669–674.
  - 14) V. G. Pushin, V. V. Kondratiev and V. N. Khachin: *Pre-transitional Phenomenon and Martensitic Transformations*, (Ekaterinburg: Ural Branch of RAS, 1998) p. 368. (in Russian).
  - 15) R. Z. Valiev, I. V. Alexandrov, Y. T. Zhu and T. C. Lowe: *J. Mater. Res.* **17** (2002) 5–8.
  - 16) Y. T. Zhu, T. C. Lowe and T. G. Langdon: *Scripta Mater.* **51** (2004) 825–829.
  - 17) Y. Liu and D. Favier: *Acta Mater.* **48** (2000) 3489–3499.
  - 18) T. Waitz, V. Kazykhanov and H. P. Karnthaler: *Acta Mater.* **52** (2004) 137.
  - 19) E. Ma: *JOM* **58** (2006) 49–53.
  - 20) L. Lu, Y. Shen, X. Chen, L. Qian and K. Lu: *Science* **304** (2004) 422–426.
  - 21) Y.-H. Zhao, J. F. Bingert, X.-Z. Liao, B.-Z. Cui, K. Han, A. V. Sergueeva, A. K. Mukherjee, R. Z. Valiev, T. G. Langdon and Y. T. Zhu: *Adv. Mater.* **18** (2006) 2949–2953.